Midlatitude Pi2 Pulsations: AFGL and ISEE Magnetometer Observations Correlated *

W.J. Hughes and H.J. Singer
Boston University

N.C. Maynard
NASA/Goddard Space Flight Center

ABSTRACT

Most spacecraft observations of the pi2 magnetic pulsations that occur at substorm onset have been made near geostationary orbit where the signal character is quite different from that seen on the ground, expecially that seen at mid-latitudes. However the ISEE spacecraft have observed pi2 pulsations in the inner magnetosphere. We report on one of these events which was also detected as a pi2 event by the AFGL midlatitude magnetometers. The event occurred when the foot of the ISEE field line was over North America. The ground and satellite signals are remarkably similar: they start and stop at the same time, have the same period and can be correlated cycle by cycle. The waves are detected in the electric field data from ISEE 1 and in the magnetic field data from both ISEE 1 and ISEE 2. Calculation of the Poynting vector at ISEE 1 shows that the energy flowed mainly westward, but that there was also a component towards the nearer (southern) ionospheric foot of the field line. The phases between the various field components measured by ISEE 1 and 2 indicate that this is a standing hydromagnetic oscillation.

(NASA-TM-84763) MIDLATITUDE Pi2 PULSATIONS: AFGL AND ISEE MAGNETOMETER OBSERVATIONS CORRELATED (NASA) 10 p HC A02/MF A01 CSCL 03B
N82-28232
Unclas
G3/90 28304

* Work supported by NASA research grant, NSG 5407.

EXTENDED FIGURE CAPTIONS

Figure 1 - shows the footpoints of ISEE 1 and 2 and also of GOES 2 and the locations of the ground observatories from which data was used. The heavy line in the ISEE footprint indicates the location of the spacecraft when the wave occurred.

Figure 2 - shows magnetometer data from the AFGL network. The data has been passed through a high pass filter (cut-off at 4 mHz or 250s) to remove DC trends. A typical pi2 wave packet is seen, the amplitude being smaller at the two southern stations. The remarkable similarity between the records is typical of this sort of pulsation.

Figure 3 - the location of the substorm onset associated with this pulsation can be approximately located by plotting hodograms from each of the stations as shown in this figure. The hodograms (H component variation plotted against D component variation) have been placed to schematically show the geographic locations of the stations. The major axes of the polarization ellipses, if extended, all intersect at a point due north of Sudbury. The GWR magnetogram (not shown) confirms that breakup occurred a little to the SW of GWR.

Figure 4 - shows the $\underset{\sim}{E}$ and $\underset{\sim}{B}$ field data from ISEE 1 & 2. The data is presented in a mean field aligned coordiante system with $\hat{z}$ along the measured background field direction. The assumption $\underset{\sim}{E}.\underset{\sim}{B} = 0$ is made in transforming the electric field. The data has been filtered in the same manner as in figure 2. The electric field from ISEE 1 (none is available from ISEE 2) is particularly well correlated with the ground data; both the amplitude and time of individual cycles match.

Figure 5 - shows the results of computing the wave Poynting vector at ISEE 1. The field aligned component, S_z, shows that energy flows back and forth along the field line, suggestive of a standing wave, but with a net energy flow in the negative $\hat{z}$ direction, towards the nearer ionosphere where presumably energy is being drained from the system by Joule heating. The transverse components, S_x and S_y, combine to give a net perpendicular energy flow westward as is indicated in the next figure.

Figure 6 - shows again the locations of the spacecraft and ground observatories, this time in an L - Local time projection. The arrow by ISEE 1 shows the direction of energy flow perpendicular to the field line. The energy flows westward with a small radially inward component. As onset occurs north of Sudbury somewhere close to GWR (see figure 3), this is consistent with energy flowing away from the substorm onset region.

Figure 7 - shows the phase relationships between the various field components measured relative to the H component at Mt. Clemens and were obtained using cross-spectral techniques. Of particular note are the phase relationships between the spacecraft measurements. The approximate 90° shift between $\underline{E}$ and $\underline{B}$ on ISEE 1 with B_y leading E_x indicates that this is an odd harmonic standing hydromagnetic oscillation of the field line. The three $\underline{B}$ components on ISEE 1 lead those on ISEE 2 by 10-40° although ISEE 2 is on larger L shells. This is extremely suggestive of a field line resonance.

CONCLUSIONS

This is the first confirmed observation of a midlatitude pi2 wave in space. We have shown that the waves are very similar on the ground and in space and very dissimilar to the geostationary orbit signature (seen on GOES 2). The event is seen over a wide range of L shells (L=2 to L=5) and over nearly 6 hours of local time. The spacecraft observations show that this is a standing wave, possibly a resonant one and that the energy flow is consistent with the usual substorm picture.

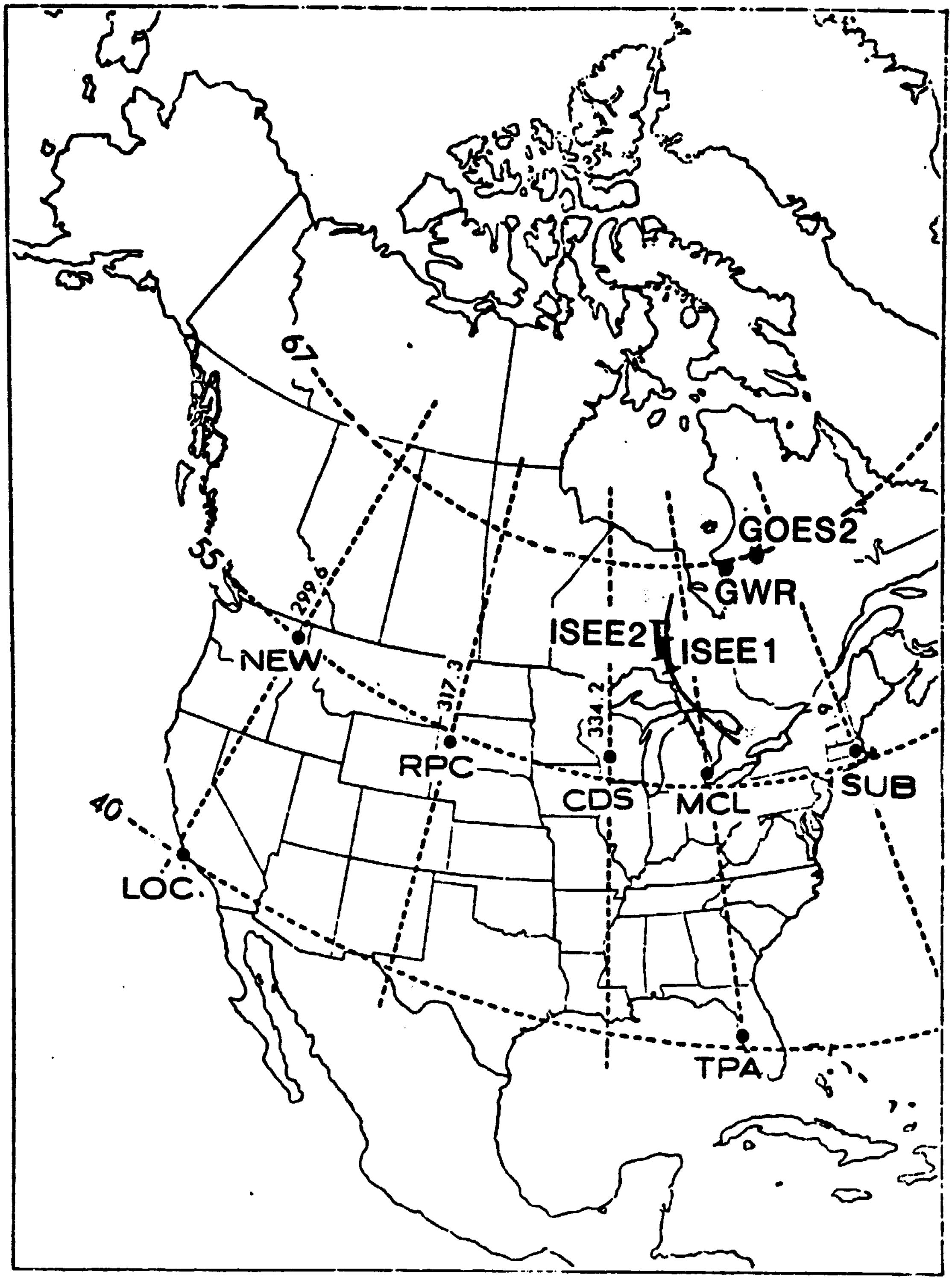
67
55
40
GOES2
GWR
ISEE2
ISEE1
299.6
NEW
317.3
RPC
334.2
CDS
MCL
SUB
LOC
TPA

Figure 1

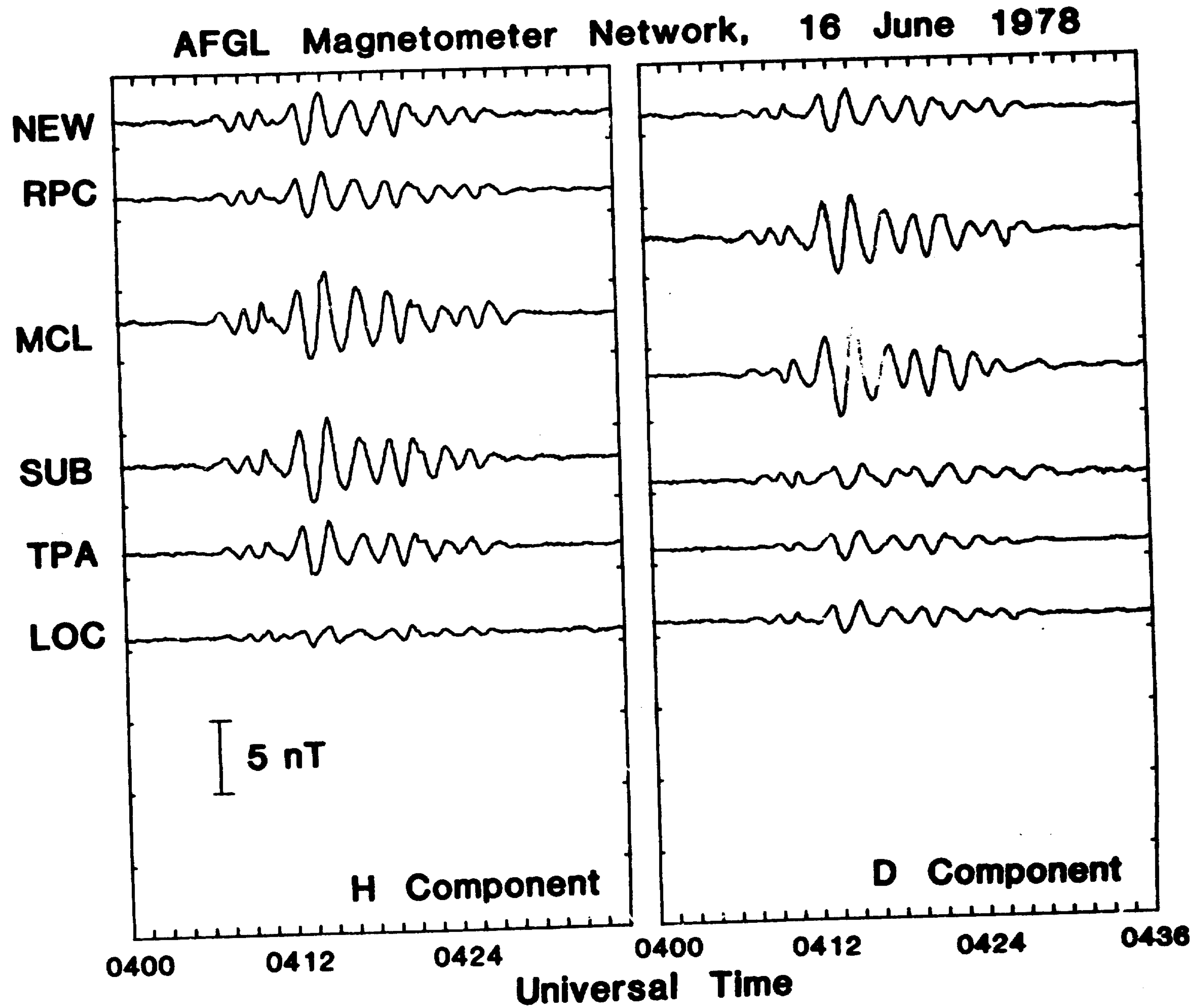
AFGL Magnetometer Network, 16 June 1978
NEW
RPC
MCL
SUB
TPA
LOC
5 nT
H Component
D Component
0400
0412
0424
0400
0412
0424
0436
Universal Time

Figure 2.

AFGL Magnetometer Network

16 June 1978, 0414–0420 UT

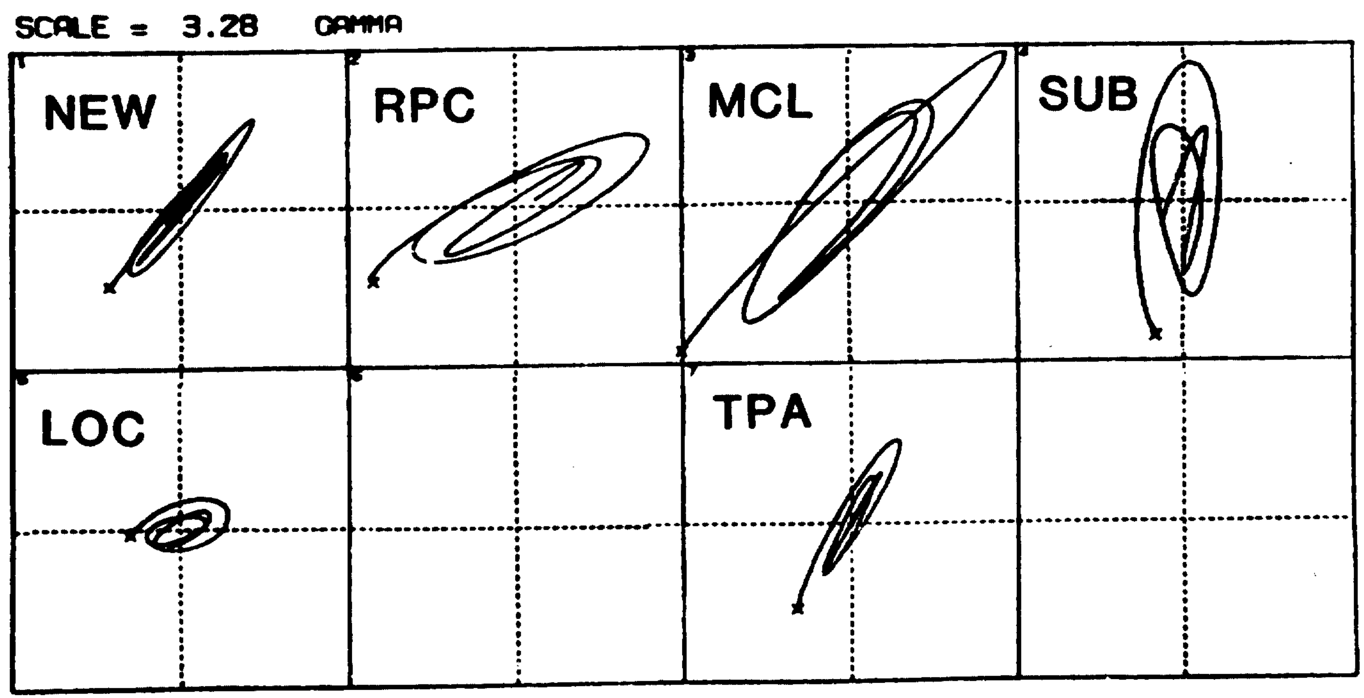

Figure 3

16 JUNE 1978

ISEE 1 & 2, E & B Fields, Field-aligned Coordinates

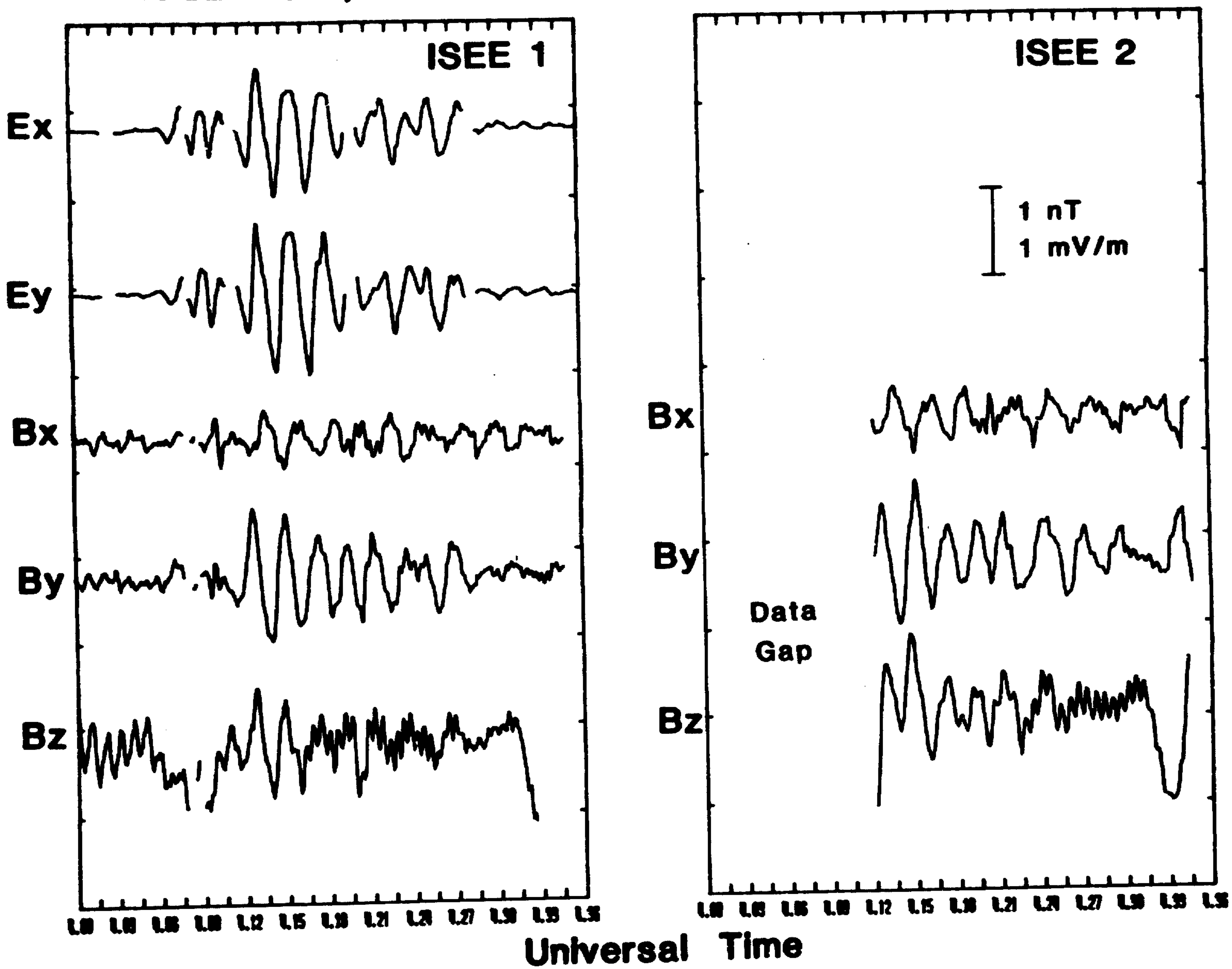

Figure 4

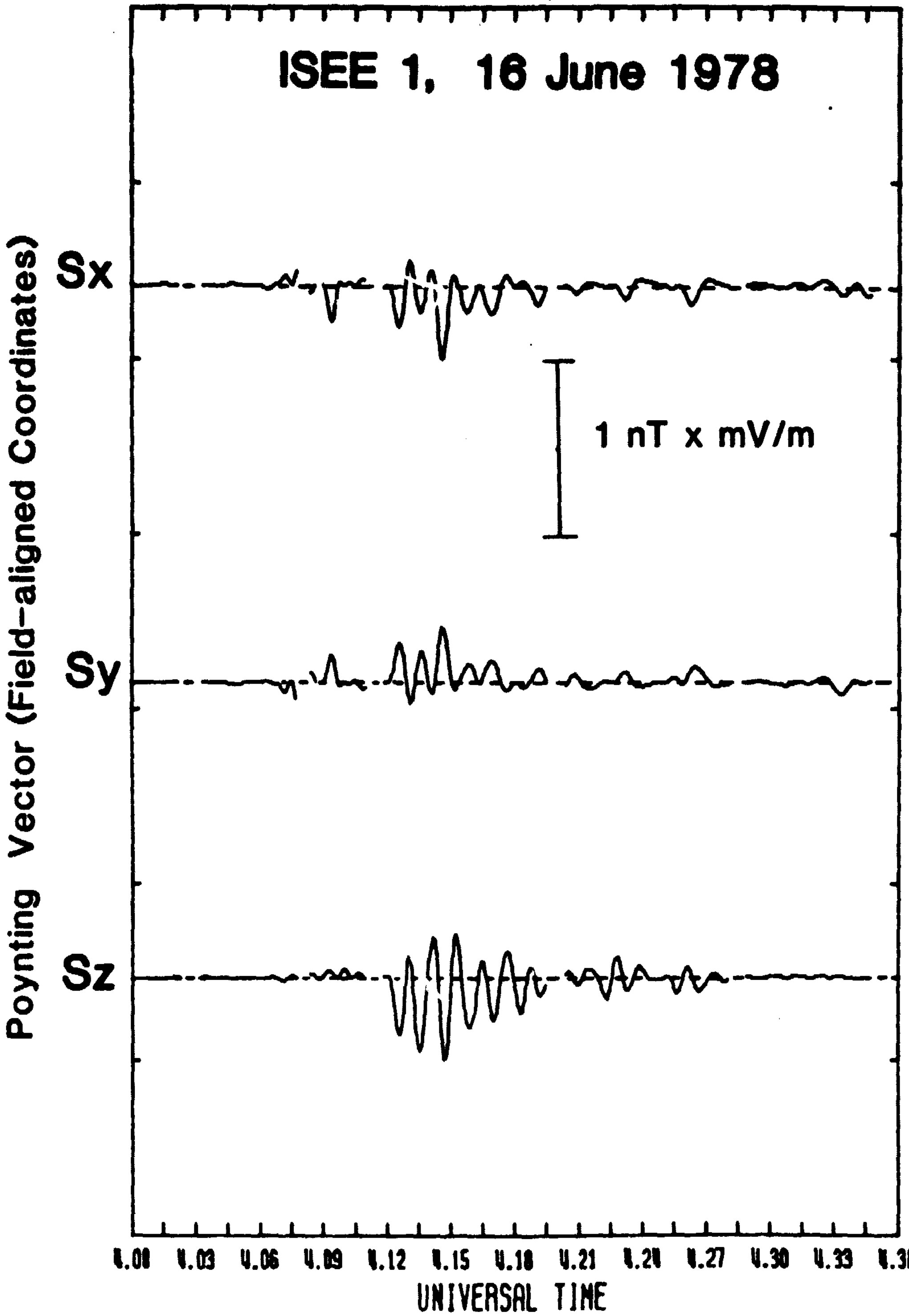
ISEE 1, 16 June 1978
Poynting Vector (Field-aligned Coordinates)
Sx
Sy
Sz
1 nT x mV/m
UNIVERSAL TIME

Figure 5

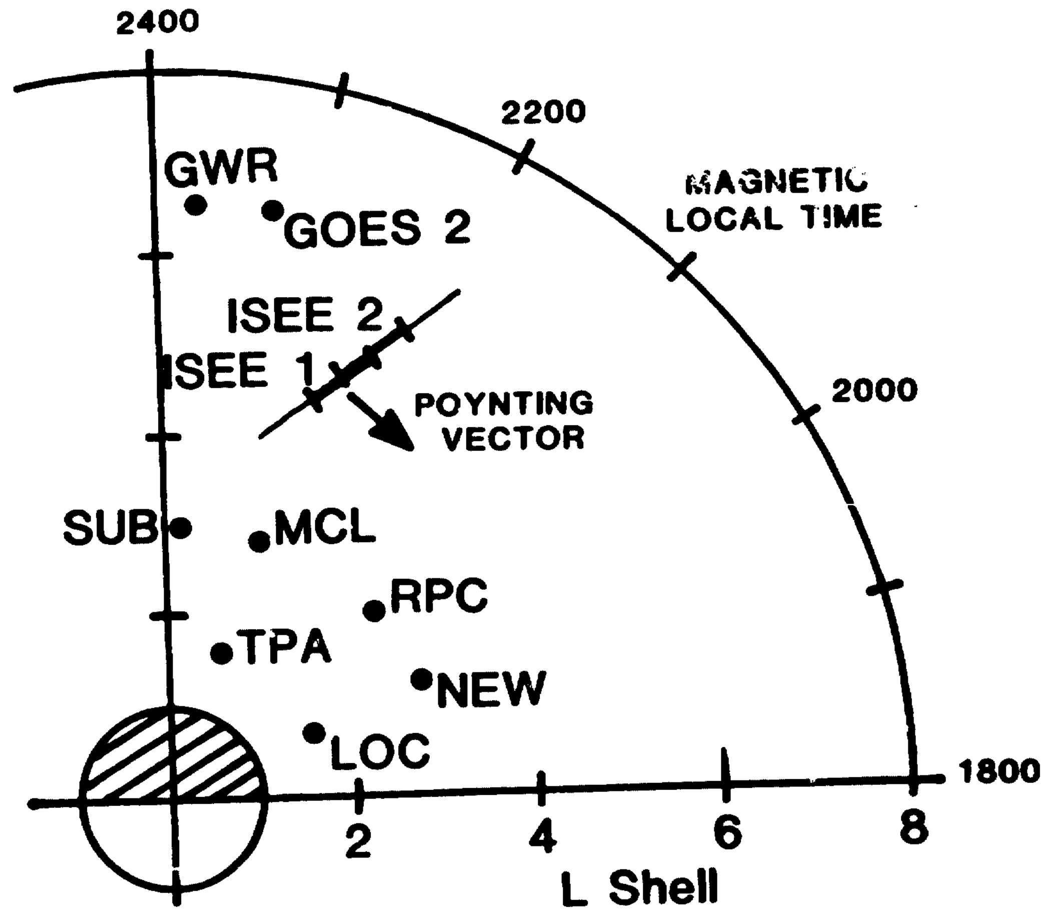
2400
2200
2000
1800
MAGNETIC
LOCAL TIME
GWR
GOES 2
ISEE 2
ISEE 1
POYNTING
VECTOR
SUB
MCL
RPC
TPA
NEW
LOC
2
4
6
8
L Shell

Figure 6

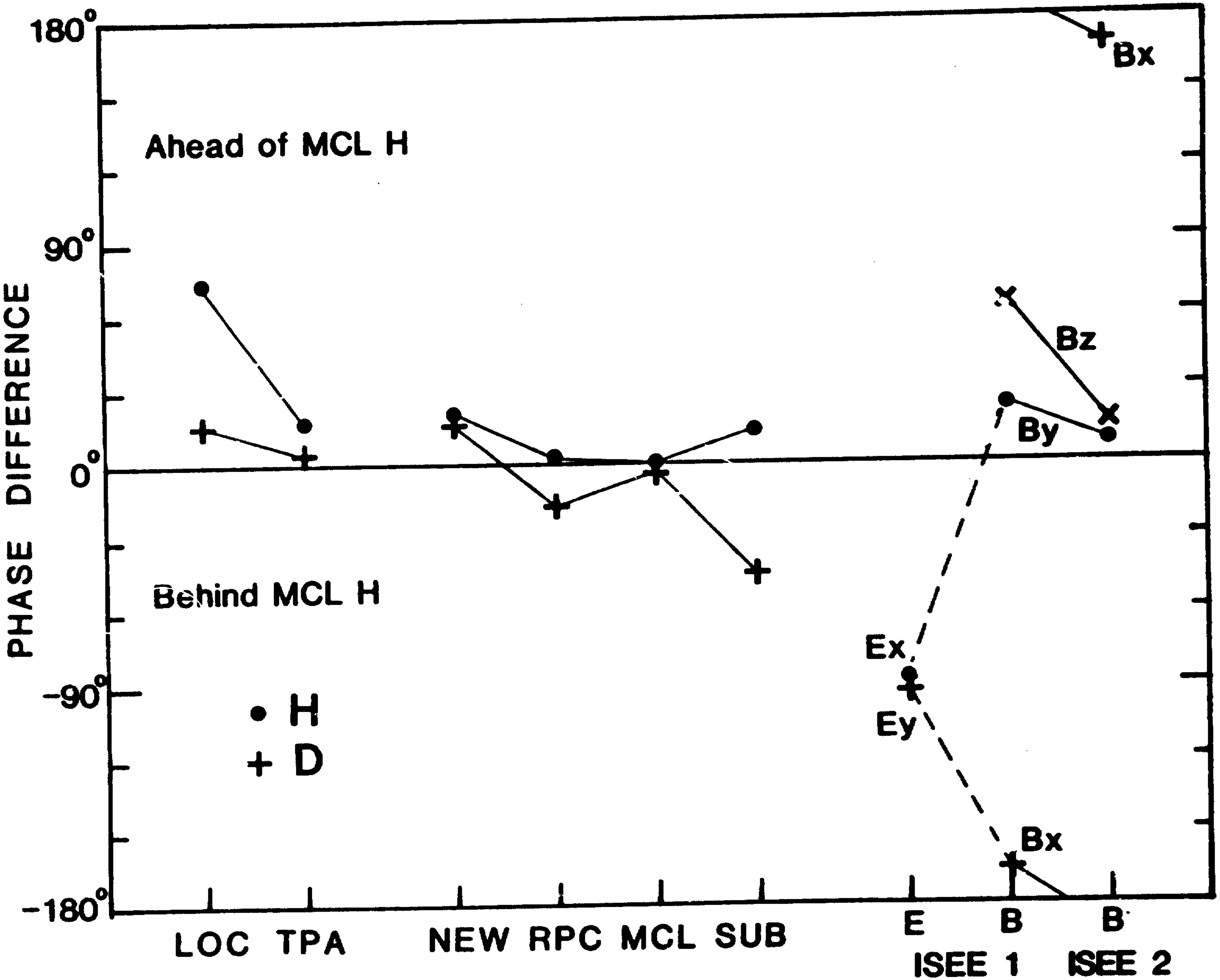
180°
90°
0°
-90°
-180°
PHASE DIFFERENCE
Ahead of MCL H
Behind MCL H
• H
+ D
Bx
Bz
By
Ex
Ey
Bx
LOC TPA
NEW RPC MCL SUB
E B B
ISEE 1 ISEE 2

Figure 7